

MIT Open Access Articles

*First Search for Exotic Z Boson Decays into
Photons and Neutral Pions in Hadron Collisions*

The MIT Faculty has made this article openly available. **Please share** how this access benefits you. Your story matters.

Citation: Aaltonen, T., et al. "First Search for Exotic Z Boson Decays into Photons and Neutral Pions in Hadron Collisions." Phys. Rev. Lett. 112, 111803 (March 2014). © 2014 American Physical Society

As Published: <http://dx.doi.org/10.1103/PhysRevLett.112.111803>

Publisher: American Physical Society

Persistent URL: <http://hdl.handle.net/1721.1/88984>

Version: Final published version: final published article, as it appeared in a journal, conference proceedings, or other formally published context

Terms of Use: Article is made available in accordance with the publisher's policy and may be subject to US copyright law. Please refer to the publisher's site for terms of use.



First Search for Exotic Z Boson Decays into Photons and Neutral Pions in Hadron Collisions

T. Aaltonen,²¹ S. Amerio,^{39b,39a} D. Amidei,³¹ A. Anastassov,^{15,w} A. Annovi,¹⁷ J. Antos,¹² G. Apollinari,¹⁵ J. A. Appel,¹⁵ T. Arisawa,⁵² A. Artikov,¹³ J. Asaadi,⁴⁷ W. Ashmanskas,¹⁵ B. Auerbach,² A. Aurisano,⁴⁷ F. Azfar,³⁸ W. Badgett,¹⁵ T. Bae,²⁵ A. Barbaro-Galtieri,²⁶ V. E. Barnes,⁴³ B. A. Barnett,²³ P. Barria,^{41c,41a} P. Bartos,¹² M. Baucé,^{39b,39a} F. Bedeschi,^{41a} S. Behari,¹⁵ G. Bellettini,^{41b,41a} J. Bellinger,⁵⁴ D. Benjamin,¹⁴ A. Beretvas,¹⁵ A. Bhatti,⁴⁵ K. R. Bland,⁵ B. Blumenfeld,²³ A. Bocci,¹⁴ A. Bodek,⁴⁴ D. Bortoletto,⁴³ J. Boudreau,⁴² A. Boveia,¹¹ L. Brigliadori,^{6b,6a} C. Bromberg,³² E. Brucken,²¹ J. Budagov,¹³ H. S. Budd,⁴⁴ K. Burkett,¹⁵ G. Busetto,^{39b,39a} P. Bussey,¹⁹ P. Butti,^{41b,41a} A. Buzatu,¹⁹ A. Calamba,¹⁰ S. Camarda,⁴ M. Campanelli,²⁸ F. Canelli,^{11,dd} B. Carls,²² D. Carlsmith,⁵⁴ R. Carosi,^{41a} S. Carrillo,^{16,m} B. Casal,^{9,k} M. Casarsa,^{48a} A. Castro,^{6b,6a} P. Catastini,²⁰ D. Cauz,^{48b,48c,48a} V. Cavaliere,²² M. Cavalli-Sforza,⁴ A. Cerri,^{26,f} L. Cerrito,^{28,r} Y. C. Chen,¹ M. Chertok,⁷ G. Chiarelli,^{41a} G. Chlachidze,¹⁵ K. Cho,²⁵ D. Chokheli,¹³ A. Clark,¹⁸ C. Clarke,⁵³ M. E. Convery,¹⁵ J. Conway,⁷ M. Corbo,^{15,z} M. Cordelli,¹⁷ C. A. Cox,⁷ D. J. Cox,⁷ M. Cremonesi,^{41a} D. Cruz,⁴⁷ J. Cuevas,^{9,y} R. Culbertson,¹⁵ N. d'Ascenzo,^{15,v} M. Datta,^{15,gg} P. de Barbaro,⁴⁴ L. Demortier,⁴⁵ M. Deninno,^{6a} M. D'Errico,^{39b,39a} F. Devoto,²¹ A. Di Canto,^{41b,41a} B. Di Ruzza,^{15,q} J. R. Dittmann,⁵ S. Donati,^{41b,41a} M. D'Onofrio,²⁷ M. Dorigo,^{48d,48a} A. Driutti,^{48b,48c,48a} K. Ebina,⁵² R. Edgar,³¹ A. Elagin,⁴⁷ R. Erbacher,⁷ S. Errede,²² B. Esham,²² S. Farrington,³⁸ J. P. Fernández Ramos,²⁹ R. Field,¹⁶ G. Flanagan,^{15,t} R. Forrest,⁷ M. Franklin,²⁰ J. C. Freeman,¹⁵ H. Frisch,¹¹ Y. Funakoshi,⁵² C. Galloni,^{41b,41a} A. F. Garfinkel,⁴³ P. Garosi,^{41c,41a} H. Gerberich,²² E. Gerchtein,¹⁵ S. Giagu,^{46a} V. Giakoumopoulou,³ K. Gibson,⁴² C. M. Ginsburg,¹⁵ N. Giokaris,³ P. Giromini,¹⁷ G. Giurgiu,²³ V. Glagolev,¹³ D. Glenzinski,¹⁵ M. Gold,³⁴ D. Goldin,⁴⁷ A. Golossanov,¹⁵ G. Gomez,⁹ G. Gomez-Ceballos,³⁰ M. Goncharov,³⁰ O. González López,²⁹ I. Gorelov,³⁴ A. T. Goshaw,¹⁴ K. Goulianos,⁴⁵ E. Gramellini,^{6a} S. Grinstein,⁴ C. Grosso-Pilcher,¹¹ R. C. Group,^{51,15} J. Guimaraes da Costa,²⁰ S. R. Hahn,¹⁵ J. Y. Han,⁴⁴ F. Happacher,¹⁷ K. Hara,⁴⁹ M. Hare,⁵⁰ R. F. Harr,⁵³ T. Harrington-Taber,^{15,n} K. Hatakeyama,⁵ C. Hays,³⁸ J. Heinrich,⁴⁰ M. Herndon,⁵⁴ A. Hocker,¹⁵ Z. Hong,⁴⁷ W. Hopkins,^{15,g} S. Hou,¹ R. E. Hughes,³⁵ U. Husemann,⁵⁵ M. Hussein,^{32,bb} J. Huston,³² G. Introzzi,^{41e,41f,41a} M. Iori,^{46b,46a} A. Ivanov,^{7,p} E. James,¹⁵ D. Jang,¹⁰ B. Jayatilaka,¹⁵ E. J. Jeon,²⁵ S. Jindariani,¹⁵ M. Jones,⁴³ K. K. Joo,²⁵ S. Y. Jun,¹⁰ T. R. Junk,¹⁵ M. Kambeitz,²⁴ T. Kamon,^{25,47} P. E. Karchin,⁵³ A. Kasmi,⁵ Y. Kato,^{37,o} W. Ketchum,^{11,hh} J. Keung,⁴⁰ B. Kilminster,^{15,dd} D. H. Kim,²⁵ H. S. Kim,²⁵ J. E. Kim,²⁵ M. J. Kim,¹⁷ S. H. Kim,⁴⁹ S. B. Kim,²⁵ Y. J. Kim,²⁵ Y. K. Kim,¹¹ N. Kimura,⁵² M. Kirby,¹⁵ K. Knoepfel,¹⁵ K. Kondo,^{52,a} D. J. Kong,²⁵ J. Konigsberg,¹⁶ A. V. Kotwal,¹⁴ M. Kreps,²⁴ J. Kroll,⁴⁰ M. Kruse,¹⁴ T. Kuhr,²⁴ M. Kurata,⁴⁹ A. T. Laasanen,⁴³ S. Lammel,¹⁵ M. Lancaster,²⁸ K. Lannon,^{35,x} G. Latino,^{41c,41a} H. S. Lee,²⁵ J. S. Lee,²⁵ S. Leo,^{41a} S. Leone,^{41a} J. D. Lewis,¹⁵ A. Limosani,^{14,s} E. Lipeles,⁴⁰ A. Lister,^{18,b} H. Liu,⁵¹ Q. Liu,⁴³ T. Liu,¹⁵ S. Lockwitz,⁵⁵ A. Loginov,⁵⁵ D. Lucchesi,^{39b,39a} A. Lucà,¹⁷ J. Lueck,²⁴ P. Lujan,²⁶ P. Lukens,¹⁵ G. Lungu,⁴⁵ J. Lys,²⁶ R. Lysak,^{12,e} R. Madrak,¹⁵ P. Maestro,^{41c,41a} S. Malik,⁴⁵ G. Manca,^{27,c} A. Manousakis-Katsikakis,³ L. Marchese,^{6a,ii} F. Margaroli,^{46a} P. Marino,^{41d,41a} M. Martínez,⁴ K. Matera,²² M. E. Mattson,⁵³ A. Mazzacane,¹⁵ P. Mazzanti,^{6a} R. McNulty,^{27,j} A. Mehta,²⁷ P. Mehtala,²¹ C. Mesropian,⁴⁵ T. Miao,¹⁵ D. Mietlicki,³¹ A. Mitra,¹ H. Miyake,⁴⁹ S. Moed,¹⁵ N. Moggi,^{6a} C. S. Moon,^{15,z} R. Moore,^{15,ee,ff} M. J. Morello,^{41d,41a} A. Mukherjee,¹⁵ Th. Muller,²⁴ P. Murat,¹⁵ M. Mussini,^{6b,6a} J. Nachtman,^{15,n} Y. Nagai,⁴⁹ J. Naganoma,⁵² I. Nakano,³⁶ A. Napier,⁵⁰ J. Nett,⁴⁷ C. Neu,⁵¹ T. Nigmanov,⁴² L. Nodulman,² S. Y. Noh,²⁵ O. Norriella,²² L. Oakes,³⁸ S. H. Oh,¹⁴ Y. D. Oh,²⁵ I. Oksuzian,⁵¹ T. Okusawa,³⁷ R. Orava,²¹ L. Ortolan,⁴ C. Pagliarone,^{48a} E. Palencia,^{9,f} P. Palni,³⁴ V. Papadimitriou,¹⁵ W. Parker,⁵⁴ G. Pauletta,^{48b,48c,48a} M. Paulini,¹⁰ C. Paus,³⁰ T. J. Phillips,¹⁴ G. Piacentino,^{41a} E. Pianori,⁴⁰ J. Pilot,⁷ K. Pitts,²² C. Plager,⁸ L. Pondrom,⁵⁴ S. Poprocki,^{15,g} K. Potamianos,²⁶ A. Pranko,²⁶ F. Prokoshin,^{13,aa} F. Ptohos,^{17,h} G. Punzi,^{41b,41a} N. Ranjan,⁴³ I. Redondo Fernández,²⁹ P. Renton,³⁸ M. Rescigno,^{46a} F. Rimondi,^{6a,a} L. Ristori,^{41a,15} A. Robson,¹⁹ T. Rodriguez,⁴⁰ S. Rolli,^{50,i} M. Ronzani,^{41b,41a} R. Roser,¹⁵ J. L. Rosner,¹¹ F. Ruffini,^{41c,41a} A. Ruiz,⁹ J. Russ,¹⁰ V. Rusu,¹⁵ W. K. Sakumoto,⁴⁴ Y. Sakurai,⁵² L. Santi,^{48b,48c,48a} K. Sato,⁴⁹ V. Saveliev,^{15,v} A. Savoy-Navarro,^{15,z} P. Schlabach,¹⁵ E. E. Schmidt,¹⁵ T. Schwarz,³¹ L. Scodellaro,⁹ F. Scuri,^{41a} S. Seidel,³⁴ Y. Seiya,³⁷ A. Semenov,¹³ F. Sforza,^{41b,41a} S. Z. Shalhout,⁷ T. Shears,²⁷ P. F. Shepard,⁴² M. Shimojima,^{49,u} M. Shochet,¹¹ I. Shreyber-Tecker,³³ A. Simonenko,¹³ K. Sliwa,⁵⁰ J. R. Smith,⁷ F. D. Snider,¹⁵ H. Song,⁴² V. Sorin,⁴ R. St. Denis,¹⁹ M. Stancari,¹⁵ D. Stentz,^{15,w} J. Strologas,³⁴ Y. Sudo,⁴⁹ A. Sukhanov,¹⁵ I. Suslov,¹³ K. Takemasa,⁴⁹ Y. Takeuchi,⁴⁹ J. Tang,¹¹ M. Tecchio,³¹ P. K. Teng,¹ J. Thom,^{15,g} E. Thomson,⁴⁰ V. Thukral,⁴⁷ D. Toback,⁴⁷ S. Tokar,¹² K. Tollefson,³² T. Tomura,⁴⁹ D. Tonelli,^{15,f} S. Torre,¹⁷ D. Torretta,¹⁵ P. Totaro,^{39a} M. Trovato,^{41d,41a} F. Ukegawa,⁴⁹ S. Uozumi,²⁵ F. Vázquez,^{16,m} G. Velev,¹⁵ C. Vellidis,¹⁵ C. Vernieri,^{41d,41a} M. Vidal,⁴³ R. Vilar,⁹ J. Vizán,^{9,cc} M. Vogel,³⁴ G. Volpi,¹⁷ P. Wagner,⁴⁰ R. Wallny,^{15,k} S. M. Wang,¹ D. Waters,²⁸ W. C. Wester III,¹⁵ D. Whiteson,^{40,d} A. B. Wicklund,²

S. Wilbur,⁷ H. H. Williams,⁴⁰ J. S. Wilson,³¹ P. Wilson,¹⁵ B. L. Winer,³⁵ P. Wittich,^{15,g} S. Wolbers,¹⁵ H. Wolfe,³⁵ T. Wright,³¹
 X. Wu,¹⁸ Z. Wu,⁵ K. Yamamoto,³⁷ D. Yamato,³⁷ T. Yang,¹⁵ U. K. Yang,²⁵ Y. C. Yang,²⁵ W.-M. Yao,²⁶ G. P. Yeh,¹⁵ K. Yi,^{15,n}
 J. Yoh,¹⁵ K. Yorita,⁵² T. Yoshida,^{37,1} G. B. Yu,¹⁴ I. Yu,²⁵ A. M. Zanetti,^{48a} Y. Zeng,¹⁴ C. Zhou,¹⁴ S. Zucchelli^{6b,6a}

(CDF Collaboration)

¹*Institute of Physics, Academia Sinica, Taipei, Taiwan 11529, Republic of China*

²*Argonne National Laboratory, Argonne, Illinois 60439, USA*

³*University of Athens, 157 71 Athens, Greece*

⁴*Institut de Física d'Altes Energies, ICREA, Universitat Autònoma de Barcelona, E-08193, Bellaterra (Barcelona), Spain*

⁵*Baylor University, Waco, Texas 76798, USA*

^{6a}*Istituto Nazionale di Fisica Nucleare Bologna, I-40127 Bologna, Italy*

^{6b}*University of Bologna, I-40127 Bologna, Italy*

⁷*University of California, Davis, Davis, California 95616, USA*

⁸*University of California, Los Angeles, Los Angeles, California 90024, USA*

⁹*Instituto de Física de Cantabria, CSIC-University of Cantabria, 39005 Santander, Spain*

¹⁰*Carnegie Mellon University, Pittsburgh, Pennsylvania 15213, USA*

¹¹*Enrico Fermi Institute, University of Chicago, Chicago, Illinois 60637, USA*

¹²*Comenius University, 842 48 Bratislava, Slovakia; Institute of Experimental Physics, 040 01 Kosice, Slovakia*

¹³*Joint Institute for Nuclear Research, RU-141980 Dubna, Russia*

¹⁴*Duke University, Durham, North Carolina 27708, USA*

¹⁵*Fermi National Accelerator Laboratory, Batavia, Illinois 60510, USA*

¹⁶*University of Florida, Gainesville, Florida 32611, USA*

¹⁷*Laboratori Nazionali di Frascati, Istituto Nazionale di Fisica Nucleare, I-00044 Frascati, Italy*

¹⁸*University of Geneva, CH-1211 Geneva 4, Switzerland*

¹⁹*Glasgow University, Glasgow G12 8QQ, United Kingdom*

²⁰*Harvard University, Cambridge, Massachusetts 02138, USA*

²¹*Division of High Energy Physics, Department of Physics, University of Helsinki, FIN-00014, Helsinki, Finland;*

Helsinki Institute of Physics, FIN-00014, Helsinki, Finland

²²*University of Illinois, Urbana, Illinois 61801, USA*

²³*The Johns Hopkins University, Baltimore, Maryland 21218, USA*

²⁴*Institut für Experimentelle Kernphysik, Karlsruhe Institute of Technology, D-76131 Karlsruhe, Germany*

²⁵*Center for High Energy Physics: Kyungpook National University, Daegu 702-701, Korea; Seoul National University, Seoul 151-742, Korea; Sungkyunkwan University, Suwon 440-746, Korea; Korea Institute of Science and Technology Information, Daejeon 305-806, Korea; Chonnam National University, Gwangju 500-757, Korea;*

Chonbuk National University, Jeonju 561-756, Korea; Ewha Womans University, Seoul 120-750, Korea

²⁶*Ernest Orlando Lawrence Berkeley National Laboratory, Berkeley, California 94720, USA*

²⁷*University of Liverpool, Liverpool L69 7ZE, United Kingdom*

²⁸*University College London, London WC1E 6BT, United Kingdom*

²⁹*Centro de Investigaciones Energéticas Medioambientales y Tecnológicas, E-28040 Madrid, Spain*

³⁰*Massachusetts Institute of Technology, Cambridge, Massachusetts 02139, USA*

³¹*University of Michigan, Ann Arbor, Michigan 48109, USA*

³²*Michigan State University, East Lansing, Michigan 48824, USA*

³³*Institution for Theoretical and Experimental Physics, ITEP, Moscow 117259, Russia*

³⁴*University of New Mexico, Albuquerque, New Mexico 87131, USA*

³⁵*The Ohio State University, Columbus, Ohio 43210, USA*

³⁶*Okayama University, Okayama 700-8530, Japan*

³⁷*Osaka City University, Osaka 558-8585, Japan*

³⁸*University of Oxford, Oxford OX1 3RH, United Kingdom*

^{39a}*Istituto Nazionale di Fisica Nucleare, Sezione di Padova, I-35131 Padova, Italy*

^{39b}*University of Padova, I-35131 Padova, Italy*

⁴⁰*University of Pennsylvania, Philadelphia, Pennsylvania 19104, USA*

^{41a}*Istituto Nazionale di Fisica Nucleare Pisa, I-56127 Pisa, Italy*

^{41b}*University of Pisa, I-56127 Pisa, Italy*

^{41c}*University of Siena, I-56127 Pisa, Italy*

^{41d}*Scuola Normale Superiore, I-56127 Pisa, Italy*

^{41e}*INFN Pavia, I-27100 Pavia, Italy,*

^{41f}*University of Pavia, I-27100 Pavia, Italy*

⁴²*University of Pittsburgh, Pittsburgh, Pennsylvania 15260, USA*

⁴³*Purdue University, West Lafayette, Indiana 47907, USA*⁴⁴*University of Rochester, Rochester, New York 14627, USA*⁴⁵*The Rockefeller University, New York, New York 10065, USA*^{46a}*Istituto Nazionale di Fisica Nucleare, Sezione di Roma 1, I-00185 Roma, Italy*^{46b}*Sapienza Università di Roma, I-00185 Roma, Italy*⁴⁷*Mitchell Institute for Fundamental Physics and Astronomy, Texas A&M University, College Station, Texas 77843, USA*^{48a}*Istituto Nazionale di Fisica Nucleare Trieste, I-33100 Udine, Italy*^{48b}*Gruppo Collegato di Udine, I-33100 Udine, Italy*^{48c}*University of Udine, I-33100 Udine, Italy*^{48d}*University of Trieste, I-34127 Trieste, Italy*⁴⁹*University of Tsukuba, Tsukuba, Ibaraki 305, Japan*⁵⁰*Tufts University, Medford, Massachusetts 02155, USA*⁵¹*University of Virginia, Charlottesville, Virginia 22906, USA*⁵²*Waseda University, Tokyo 169, Japan*⁵³*Wayne State University, Detroit, Michigan 48201, USA*⁵⁴*University of Wisconsin, Madison, Wisconsin 53706, USA*⁵⁵*Yale University, New Haven, Connecticut 06520, USA*

(Received 14 November 2013; published 20 March 2014)

A search for forbidden and exotic Z boson decays in the diphoton mass spectrum is presented for the first time in hadron collisions, based on data corresponding to 10.0 fb^{-1} of integrated luminosity from proton-antiproton collisions at $\sqrt{s} = 1.96 \text{ TeV}$ collected by the CDF experiment. No evidence of signal is observed, and 95% credibility level Bayesian upper limits are set on the branching ratios of decays of the Z boson to a photon and neutral pion (which is detected as a photon), a pair of photons, and a pair of neutral pions. The observed branching ratio limits are 2.01×10^{-5} for $Z \rightarrow \pi^0 \gamma$, 1.46×10^{-5} for $Z \rightarrow \gamma \gamma$, and 1.52×10^{-5} for $Z \rightarrow \pi^0 \pi^0$. The $Z \rightarrow \pi^0 \gamma$ and $Z \rightarrow \gamma \gamma$ limits improve the most stringent results from other experiments by factors of 2.6 and 3.6, respectively. The $Z \rightarrow \pi^0 \pi^0$ branching ratio limit is the first experimental result on this decay.

DOI: 10.1103/PhysRevLett.112.111803

PACS numbers: 13.38.Dg, 12.60.-i, 14.70.Hp

Properties of the W and Z bosons have been studied extensively in collider experiments. Most knowledge about these particles from hadron colliders, however, comes from decays involving leptons [1]. Although the hadronic decay modes of the W and Z bosons dominate, identifying a W or Z boson resonance from the quark-antiquark final state is challenging at hadron colliders due to large backgrounds and poor jet energy resolution. It is therefore appealing to consider rare $V \rightarrow P + \gamma$ decays, where V is a weak vector boson and P is a pseudoscalar meson. To complement the search for $W^\pm \rightarrow \pi^\pm \gamma$ decays performed previously at CDF [2], we present a new search for $Z \rightarrow \pi^0 \gamma$ decays. This decay offers a unique opportunity to reconstruct the Z boson from an isolated hadron [3], rather than from its decay to either a lepton pair or a quark-antiquark pair, and it is sensitive to couplings of the Z boson to quarks and the photon [4].

The standard model (SM) branching ratio prediction for $Z \rightarrow \pi^0 \gamma$ ranges between 10^{-12} and 10^{-9} [5], which is too small for such a process to be detected at the Tevatron. Nonetheless, evidence of a signal may indicate physics beyond the SM, and the absence of a signal would improve the current experimental upper bounds on the $Z \rightarrow \pi^0 \gamma$ branching ratio. Furthermore, an experimental limit on $\mathcal{B}(Z \rightarrow \pi^0 \gamma)$ would improve upper bounds for the pion transition form factor, which describes the $\pi^0 \rightarrow \gamma \gamma^*$

transition. Measurements of this factor by the *BABAR* experiment were found to be higher than the predictions of perturbative quantum chromodynamics for the momentum transfer (Q^2) range $15\text{--}34 \text{ GeV}^2$ [6]. Theoretical efforts since then have attempted to explain this discrepancy, some using experimental $\mathcal{B}(Z \rightarrow \pi^0 \gamma)$ upper limits as an additional constraint at higher Q^2 [7].

In this search for $Z \rightarrow \pi^0 \gamma$ decays, the π^0 and the γ have similar experimental signatures in the CDF II detector. It is therefore natural to extend the search to include the decays $Z \rightarrow \gamma \gamma$ and $Z \rightarrow \pi^0 \pi^0$, which are quantum mechanically forbidden due to the conservation of angular momentum applied to identical final-state particles (thus violating the spin-statistics theorem) [3,8]. The $Z \rightarrow \gamma \gamma$ decay was studied in the past by experiments at the Large Electron-Positron (LEP) collider [9–11], and the resulting limits on the $Z \rightarrow \gamma \gamma$ branching ratio have been used [12] to constrain possible small violations of Bose-Einstein statistics, complementing other similar analyses [13]. The $Z \rightarrow \gamma \gamma$ decay is also considered a promising process for discovery of physics beyond the SM that allows for noncommutative space-time [14].

The most stringent existing experimental limits on the $Z \rightarrow \pi^0 \gamma$ and $Z \rightarrow \gamma \gamma$ branching ratios come from LEP experiments [1]. Specifically, the L3 experiment set a 95% confidence level limit of 5.2×10^{-5} on the branching ratio

of both the $Z \rightarrow \pi^0\gamma$ and $Z \rightarrow \gamma\gamma$ decay modes [9]. Though the experimental search for these decays is challenging due to their small branching ratios, the abundance of Z bosons produced in high-energy hadron collisions at CDF [15] (about 4 times the number of Z bosons produced at LEP [16]) allows an improvement of the existing limits. The intensive search for the SM Higgs boson in the diphoton decay mode [17] has led to dedicated data analysis techniques that can be directly applied to $Z \rightarrow \pi^0\gamma$, $Z \rightarrow \gamma\gamma$, and $Z \rightarrow \pi^0\pi^0$ searches. No limits on the branching ratios of these decay modes from experiments in hadron collisions have been reported to date. In this Letter, we present a search for $Z \rightarrow \pi^0\gamma$, $Z \rightarrow \gamma\gamma$, and $Z \rightarrow \pi^0\pi^0$ decays using the full CDF diphoton data set, corresponding to an integrated luminosity of 10.0 fb^{-1} .

The CDF II detector [18] is used to identify photon candidate events produced in $p\bar{p}$ collisions at $\sqrt{s} = 1.96 \text{ TeV}$. The silicon vertex tracker [19] and the central outer tracker [20], contained within a 1.4 T axial magnetic field, measure the trajectories (tracks) of charged particles and determine their momenta. Particles that pass through the tracking volume reach the electromagnetic (EM) and hadronic calorimeters [21], which are divided into two regions: central ($|\eta| < 1.1$) [22] and forward ($1.1 < |\eta| < 3.6$). The EM calorimeters contain fine-grained shower maximum detectors [23], which measure the shower shape and centroid position in the two dimensions transverse to the direction of the shower development.

Events having two isolated EM showers with no associated tracks are selected by a three-level on-line event-selection system (trigger) that requires an isolated cluster of energy deposited in the EM calorimeter with transverse energy $E_T > 25 \text{ GeV}$ [24]. The trigger efficiency for events accepted into the final sample is determined from simulated events and found to be $(99.8 \pm 1.0)\%$ [17].

A neural network (NN) technique is used to reconstruct the two highest- E_T photon candidates in the event with $E_T > 15 \text{ GeV}/c$ in the fiducial region of the central EM calorimeter ($|\eta| < 1.05$). This selection was developed in the SM $H \rightarrow \gamma\gamma$ analysis at CDF [17]. The NN selection is optimized for the identification of high- E_T central photons and the rejection of the dominant background from jets. This selection also identifies neutral pions from the Z boson signal with high efficiency. For $Z \rightarrow \pi^0\gamma$ or $Z \rightarrow \pi^0\pi^0$ decays, the π^0 is isolated (not contained in a jet) and decays about 99% of the time into a pair of photons. Because of the high momentum (on average $45 \text{ GeV}/c$) of the π^0 from a Z boson decay, the photon pair is usually produced with a sufficiently narrow opening angle such that the two photons appear in the central shower-maximum detector and the central EM calorimeter as a single EM shower. Neutral pions from a Z decay then have nearly the same signature as an isolated photon, with only a slightly smaller photon identification efficiency. Therefore, any evidence of a signal in the diphoton data could indicate the identification

of an isolated photon and a neutral pion, a pair of isolated photons, or a pair of neutral pions.

Simulated events from the PYTHIA Monte Carlo (MC) generator [25] are used to predict the diphoton mass ($m_{\gamma\gamma}$) shape and the product of the efficiency and detector acceptance (ϵA) of the signal. PYTHIA version 6.2.16 is used with the CTEQ5L [26] parton distribution function set and an underlying event configuration tuned to CDF data [27]. We generate Z bosons inclusively with PYTHIA using a relativistic Breit-Wigner mass distribution for the production and an angular distribution for the decay in the Z rest frame corresponding to the spin transition $1 \rightarrow (1/2, 1/2)$. Since PYTHIA does not model the $Z \rightarrow \pi^0\gamma$, $Z \rightarrow \gamma\gamma$, and $Z \rightarrow \pi^0\pi^0$ decay modes, the decay products in PYTHIA are taken to be neutrinos (assumed massless) and afterward treated artificially as photons in the detector simulation; the events are then weighted by factors that transform the original angular distribution to one appropriate for the spin transitions $1 \rightarrow (0, 1)$ and $1 \rightarrow (1, 1)$, which correspond to the $Z \rightarrow \pi^0\gamma$ and $Z \rightarrow \gamma\gamma$ decay modes, respectively. The weighting factors are 1 for $Z \rightarrow \pi^0\gamma$ decays and $(a - \cos^2\vartheta)/(b + \cos^2\vartheta)$ for $Z \rightarrow \gamma\gamma$ decays, where ϑ is the angle between the proton momentum and the momentum of each decay product in the Z boson rest frame. For $Z \rightarrow \pi^0\pi^0$ decays, we use the same weighting factor as for $Z \rightarrow \gamma\gamma$ decays, assuming a nonzero orbital angular momentum for the pion pair in the final state. The constants $a = 1.16$ and $b = 1.32$ are derived from the PYTHIA spin-density matrix of the Z boson, which accurately describes the angular distributions of $Z \rightarrow e^+e^-$ decays measured with the CDF II detector [28]. The events are then processed through the CDF II detector and trigger simulation and event reconstruction software [29]. The final weighted samples simulate the Z boson production and decay properties, including polarization, and properly model properties that affect the detector acceptance.

To correctly model the efficiency for reconstructing $Z \rightarrow \pi^0\gamma$ and $Z \rightarrow \pi^0\pi^0$ decays, an additional weight is applied to the simulated signal events based on the ratio of the π^0 to γ NN selection efficiencies. Because of the small opening angle of the photon pair from the decay of a π^0 , the NN selection efficiency for an isolated π^0 is slightly smaller than that for an isolated γ . These NN efficiencies, shown in Fig. 1, are obtained using a special-purpose MC event generator that produces single particles with a flat E_T spectrum and does not account for the underlying event. The π^0/γ efficiency weights are applied to the simulated events on an event-by-event basis as a function of the generated E_T , once for the $Z \rightarrow \pi^0\gamma$ decay and twice for the $Z \rightarrow \pi^0\pi^0$ decay. As the decay products from the Z boson have a generated E_T distribution that peaks around 45 GeV , the weights reduce the overall reconstruction efficiency for $Z \rightarrow \pi^0\gamma$ ($Z \rightarrow \pi^0\pi^0$) decays by about 2% (4%) relative to $Z \rightarrow \gamma\gamma$ decays.

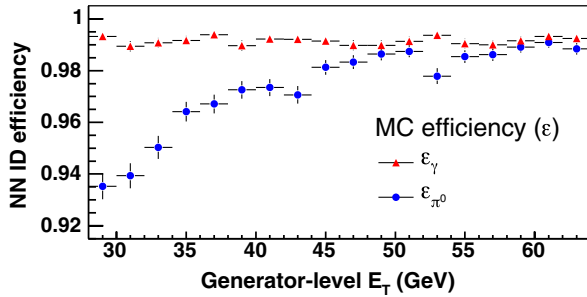


FIG. 1 (color online). Comparison of the γ and π^0 NN selection efficiencies, obtained using the special-purpose MC event generator. The efficiency is shown as a function of the generator-level E_T .

In addition to the angle and efficiency weights applied to the simulated signal samples, events from these simulated samples are further weighted such that the distribution of the number of reconstructed vertices for the sample is the same as that observed in the diphoton data. This has a negligible effect on the diphoton mass resolution. We then assume the same $m_{\gamma\gamma}$ shape for each signal process, which is justified because the mean and width of the invariant mass for each process agree to within 1%. The resulting Z boson signal has a natural width of 2.5 GeV, and is smeared by an additional 2.4 GeV due to the EM calorimeter resolution. A signal region of $80 < m_{\gamma\gamma} < 102$ GeV/ c^2 is defined, which contains 90% of the simulated signal events. Corrections to the NN selection efficiency due to imperfections in the detector simulation are also applied. These corrections are derived using electrons from $Z \rightarrow e^+e^-$ decays by comparing the selection efficiencies obtained from the detector simulation to the selection efficiencies measured in the data [30]. The products of the efficiency and detector acceptance (ϵA) for the diphoton

selection in the 80–102 GeV/ c^2 signal region, along with the associated systematic uncertainties, are $(5.67 \pm 0.42)\%$, $(7.80 \pm 0.56)\%$, and $(7.50 \pm 0.61)\%$ for the $Z \rightarrow \pi^0\gamma$, $Z \rightarrow \gamma\gamma$, and $Z \rightarrow \pi^0\pi^0$ decay modes, respectively. The $Z \rightarrow \pi^0\gamma$ decay has a lower value due primarily to its different angular distribution compared to that of $Z \rightarrow \pi^0\pi^0$ and $Z \rightarrow \pi^0\gamma$ decays.

The decay of the Z boson into $\pi^0\gamma$, $\gamma\gamma$, or $\pi^0\pi^0$ would appear as a narrow peak in the invariant mass distribution of the two reconstructed photons. The dominant backgrounds are a resonant Drell-Yan (DY) component (about 2%), which consists primarily of $Z \rightarrow e^+e^-$ decays [31], and a nonresonant component (about 98%). An inclusive $Z \rightarrow e^+e^-$ PYTHIA MC sample is used to model the DY background component, in which a pair of electrons pass the diphoton selection with $\epsilon A = (1.11 \pm 0.02) \times 10^{-5}$ in the signal region. The expected DY yield in this region is 55 ± 5 events. The dominant, nonresonant background is composed mostly (about 2/3) of events where one or two jets are identified as a reconstructed photon, denoted respectively as the γj and jj backgrounds. The remainder of the nonresonant background arises from QCD processes that produce two real photons in the hard interaction, denoted as the $\gamma\gamma$ background. The total nonresonant background prediction is estimated from a fit to the DY-subtracted data using a binned log-likelihood method. The data are fit to an exponential multiplied by a second-degree polynomial in the region 60–200 GeV/ c^2 , with the signal region window excluded from the fit. The predicted background in the signal region is obtained by interpolating the fit into this region. The fit to the data is shown in Fig. 2(a), where 2452 ± 66 events are expected in the signal region. The uncertainty on this background (2.7%) arises from the propagation of the parameter uncertainties in the fit to the event yield in the signal region. Figure 2(b) compares

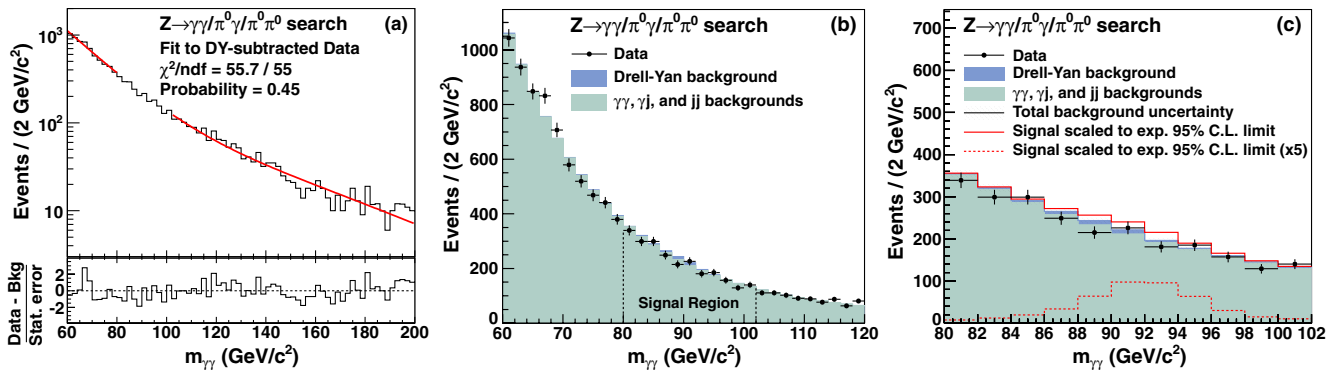


FIG. 2 (color online). (a) The diphoton mass distribution of the DY-subtracted data with the fit results overlaid. The gap in the fit function represents the excluded signal region. The lower subfigure shows the difference between the data and background predictions for the full 60–200 GeV/ c^2 region, divided by the statistical uncertainty from the background prediction. (b) The diphoton mass distribution of the Drell-Yan and nonresonant ($\gamma\gamma$, γj , and jj) backgrounds, compared to the data in the region 60–120 GeV/ c^2 , which includes part of the fit region along with the 80–102 GeV/ c^2 signal region. (c) The same distributions as (b), but for the signal region alone. Overlaid on the background is the predicted signal shape (solid line), scaled to the expected 95% C.L. upper limit. For better visibility, the same signal shape is also shown along the horizontal axis multiplied by 5 (dashed line).

TABLE I. Number of events expected in the 80–102 GeV/ c^2 signal region for the Drell-Yan and nonresonant ($\gamma\gamma$, γj , and jj) backgrounds, along with systematic uncertainties. The total background and the corresponding number of observed events in the data are also given.

Background process	Number of events
Drell-Yan	55 ± 5
$\gamma\gamma$, γj , and jj	2452 ± 66
Total background	2507 ± 66
Data	2419

the Drell-Yan and nonresonant backgrounds to the data for the region $60 < m_{\gamma\gamma} < 120$ GeV/ c^2 . An excess of events is visible near $m_{\gamma\gamma} = 67$ GeV/ c^2 . Although this mass region is not the subject of this search, we verify that the statistical significance of this excess is less than 2σ after accounting for the look-elsewhere effect [32]. Table I provides the background and data yields in the signal region.

The dominant uncertainty in the analysis is from the uncertainty in the nonresonant background prediction, as described above. The largest systematic uncertainties on the expected number of signal events arise from the integrated luminosity measurement (6%) and the measured Z boson cross section (6%) [15], which are also uncertainties applied to the $Z \rightarrow e^+e^-$ MC modeling. Uncertainties on the efficiency and detector acceptance of the signal come from varying the parton distribution functions used in PYTHIA (5%) [33] and the parameters controlling the amount of initial- and final-state radiation from the parton shower model of PYTHIA (3%) [34]; they also include uncertainties in the NN photon selection efficiency (4%), the π^0/γ efficiency weight (2% per π^0), the trigger efficiency (1%), and the EM energy scale (less than 1%). Uncertainties on the efficiency and detector acceptance of $Z \rightarrow e^+e^-$ events come from the electron misidentification rate (2%) and the trigger efficiency (1%); other uncertainties on ϵA for $Z \rightarrow e^+e^-$ events are negligible.

No evidence of a narrow peak or any other anomalous structure is visible in the signal region of the diphoton mass spectrum, and we calculate upper limits on each of the $Z \rightarrow \pi^0\gamma$, $Z \rightarrow \gamma\gamma$, and $Z \rightarrow \pi^0\pi^0$ branching ratios. Because the three decay modes are nearly indistinguishable in the detector, we set a limit on the branching ratio of each decay mode independently, assuming the other decay modes are not present. We calculate a Bayesian credibility level (C.L.) limit based on a Poisson binned likelihood constructed from each bin in the signal region (80–102 GeV/ c^2 , with a 2 GeV/ c^2 bin width) of the background, data, and signal mass distributions. The background distribution is scaled to the expected number of events in the signal region and the signal distribution is scaled based on the experimental total cross section for Z boson production (7353 pb [15]), the

TABLE II. Upper limits at 95% C.L. on the $Z \rightarrow \gamma\gamma$, $Z \rightarrow \pi^0\gamma$, and $Z \rightarrow \pi^0\pi^0$ branching ratios. Each upper limit is based on the assumption that the Z boson decays through the corresponding process.

Signal process	95% C.L. limits ($\times 10^{-5}$)					Observed
	Expected					
	-2σ	-1σ	Median	$+1\sigma$	$+2\sigma$	
$B(Z \rightarrow \pi^0\gamma)$	1.24	1.68	2.34	3.29	4.54	2.01
$B(Z \rightarrow \gamma\gamma)$	0.87	1.21	1.72	2.40	3.34	1.46
$B(Z \rightarrow \pi^0\pi^0)$	0.94	1.28	1.76	2.52	3.39	1.52

integrated luminosity of the data sample, and the value of ϵA for the signal region. We assume that the signal branching ratio can have any non-negative value with equal prior probability. We integrate over the systematic uncertainties, each assumed to be described by a Gaussian prior probability density truncated to avoid unphysical values. A 95% C.L. limit is determined such that 95% of the posterior density for the branching ratio falls below the limit [1]. For comparison, thousands of simulated experiments are also performed, based on expected backgrounds. The median limit for these trials is the expected limit, and the region where 68% (95%) of the trials lie around the median is the 1σ (2σ) expected region. Table II provides the expected and observed 95% C.L. limits on the $Z \rightarrow \pi^0\gamma$, $Z \rightarrow \gamma\gamma$, and $Z \rightarrow \pi^0\pi^0$ branching ratios. Figure 2(c) shows the $m_{\gamma\gamma}$ distributions for the data and background in the signal region, with the signal shape scaled to the expected limit.

This Letter presents the most sensitive search to date for forbidden and exotic decays of the Z boson to a neutral pion and photon, a pair of photons, and a pair of neutral pions. We search for a narrow resonance in the diphoton mass spectrum around 91 GeV/ c^2 using the full diphoton data collected by the CDF II detector at the Tevatron. No significant evidence of a resonance is found in the data. Upper bounds on the signal branching ratios are determined, resulting in observed 95% C.L. limits of 2.01×10^{-5} , 1.46×10^{-5} , and 1.52×10^{-5} for $Z \rightarrow \pi^0\gamma$, $Z \rightarrow \gamma\gamma$, and $Z \rightarrow \pi^0\pi^0$, respectively. The $Z \rightarrow \pi^0\gamma$ and $Z \rightarrow \gamma\gamma$ limits are more sensitive by factors of 2.6 and 3.6, respectively, than the most stringent limits available. The $Z \rightarrow \pi^0\pi^0$ limit is the first experimental result on this decay.

We thank the Fermilab staff and the technical staffs of the participating institutions for their vital contributions. This work was supported by the U.S. Department of Energy and National Science Foundation; the Italian Istituto Nazionale di Fisica Nucleare; the Ministry of Education, Culture, Sports, Science and Technology of Japan; the Natural Sciences and Engineering Research Council of Canada; the National Science Council of the Republic of China; the Swiss National Science Foundation; the A.P. Sloan

Foundation; the Bundesministerium für Bildung und Forschung, Germany; the Korean World Class University Program, the National Research Foundation of Korea; the Science and Technology Facilities Council and the Royal Society, United Kingdom; the Russian Foundation for Basic Research; the Ministerio de Ciencia e Innovación, and Programa Consolider-Ingenio 2010, Spain; the Slovak R&D Agency; the Academy of Finland; the Australian Research Council (ARC); and the EU community Marie Curie Fellowship Contract No. 302103.

^aDeceased.

^bVisitor from University of British Columbia, Vancouver, BC V6T 1Z1, Canada.

^cVisitor from Istituto Nazionale di Fisica Nucleare, Sezione di Cagliari, 09042 Monserrato (Cagliari), Italy.

^dVisitor from University of California Irvine, Irvine, CA 92697, USA.

^eVisitor from Institute of Physics, Academy of Sciences of the Czech Republic, 182 21, Czech Republic.

^fVisitor from CERN, CH-1211 Geneva, Switzerland.

^gVisitor from Cornell University, Ithaca, NY 14853, USA.

^hVisitor from University of Cyprus, Nicosia CY-1678, Cyprus.

ⁱVisitor from Office of Science, U.S. Department of Energy, Washington, DC 20585, USA.

^jVisitor from University College Dublin, Dublin 4, Ireland.

^kVisitor from ETH, 8092 Zürich, Switzerland.

^lVisitor from University of Fukui, Fukui City, Fukui Prefecture, Japan 910-0017.

^mVisitor from Universidad Iberoamericana, Lomas de Santa Fe, México, C.P. 01219, Distrito Federal.

ⁿVisitor from University of Iowa, Iowa City, IA 52242, USA.

^oVisitor from Kinki University, Higashi-Osaka City, Japan 577-8502.

^pVisitor from Kansas State University, Manhattan, KS 66506, USA.

^qVisitor from Brookhaven National Laboratory, Upton, NY 11973, USA.

^rVisitor from Queen Mary, University of London, London, E1 4NS, United Kingdom.

^sVisitor from University of Melbourne, Victoria 3010, Australia.

^tVisitor from Muons, Inc., Batavia, IL 60510, USA.

^uVisitor from Nagasaki Institute of Applied Science, Nagasaki 851-0193, Japan.

^vVisitor from National Research Nuclear University, Moscow 115409, Russia.

^wVisitor from Northwestern University, Evanston, IL 60208, USA.

^xVisitor from University of Notre Dame, Notre Dame, IN 46556, USA.

^yVisitor from Universidad de Oviedo, E-33007 Oviedo, Spain.

^zVisitor from CNRS-IN2P3, Paris, F-75205 France.

^{aa}Visitor from Universidad Tecnica Federico Santa Maria, 110v Valparaiso, Chile.

^{bb}Visitor from The University of Jordan, Amman 11942, Jordan.

^{cc}Visitor from Universite catholique de Louvain, 1348 Louvain-La-Neuve, Belgium.

^{dd}Visitor from University of Zürich, 8006 Zürich, Switzerland.

^{ee}Visitor from Massachusetts General Hospital, Boston, MA 02114 USA.

^{ff}Visitor from Harvard Medical School, Boston, MA 02114 USA.

^{gg}Visitor from Hampton University, Hampton, VA 23668, USA.

^{hh}Visitor from Los Alamos National Laboratory, Los Alamos, NM 87544, USA.

ⁱⁱVisitor from Università degli Studi di Napoli Federico I, I-80138 Napoli, Italy.

- [1] J. Beringer *et al.* (Particle Data Group), *Phys. Rev. D* **86**, 010001 (2012) and 2013 partial update for the 2014 edition.
- [2] T. Aaltonen *et al.* (CDF Collaboration), *Phys. Rev. D* **85**, 032001 (2012).
- [3] M. Jacob and T. T. Wu, *Phys. Lett. B* **232**, 529 (1989).
- [4] L. Arnellos, W. J. Marciano, and Z. Parsa, *Nucl. Phys. B* **196**, 378 (1982).
- [5] N. G. Deshpande, P. B. Pal, and F. I. Olness, *Phys. Lett. B* **241**, 119 (1990); K. Hikasa, *Mod. Phys. Lett. A* **05**, 1801 (1990); A. V. Manohar, *Phys. Lett. B* **244**, 101 (1990); T. N. Pham and X. Y. Pham, *Phys. Lett. B* **247**, 438 (1990); G. B. West, *Mod. Phys. Lett. A* **05**, 2281 (1990); B.-L. Young, *Phys. Rev. D* **42**, 2396 (1990); T. Schröder, *Europhys. Lett.* **12**, 497 (1990); D. Chatterjee and S. Ghosh, *Z. Phys. C* **50**, 103 (1991); S. Maitra and P. Mukhopadhyay, *Nuovo Cimento Soc. Ital. Fis.* **107A**, 157 (1994); L. Micu, *Phys. Rev. D* **53**, 5318 (1996).
- [6] B. Aubert *et al.* (BABAR Collaboration), *Phys. Rev. D* **80**, 052002 (2009).
- [7] E. R. Arriola and W. Broniowski, *Phys. Rev. D* **81**, 094021 (2010); T. N. Pham and X. Y. Pham, *Int. J. Mod. Phys. A* **26**, 4125 (2011).
- [8] L. D. Landau, *Dokl. Akad. Nauk SSSR* **60**, 207 (1948); C. N. Yang, *Phys. Rev.* **77**, 242 (1950).
- [9] M. Acciarri *et al.* (L3 Collaboration), *Phys. Lett. B* **353**, 136 (1995).
- [10] P. Abreu *et al.* (DELPHI Collaboration), *Phys. Lett. B* **327**, 386 (1994).
- [11] M. Z. Akrawy *et al.* (OPAL Collaboration), *Phys. Lett. B* **257**, 531 (1991).
- [12] A. Yu. Ignatiev, G. C. Joshi, and M. Matsuda, *Mod. Phys. Lett. A* **11**, 871 (1996); S. N. Gninenko, A. Yu. Ignatiev, and V. A. Matveev, *Int. J. Mod. Phys. A* **26**, 4367 (2011).
- [13] O. W. Greenberg and R. N. Mohapatra, *Phys. Rev. D* **39**, 2032 (1989); D. DeMille, D. Budker, N. Derr, and E. Deveney, *Phys. Rev. Lett.* **83**, 3978 (1999); R. C. Hilborn, *Phys. Rev. A* **65**, 032104 (2002).
- [14] I. Hinchliffe, N. Kersting, and Y. L. Ma, *Int. J. Mod. Phys. A* **19**, 179 (2004); W. Behr, N. G. Deshpande, G. Duplančić, P. Schupp, J. Trampetić, and J. Wess, *Eur. Phys. J. C* **29**, 441 (2003); G. Duplančić, P. Schupp, and J. Trampetić, *Eur. Phys. J. C* **32**, 141 (2003); M. Burić, D. Latas, V. Radovanović, and J. Trampetić, *Phys. Rev. D* **75**, 097701 (2007); J. Trampetić,

- Fortschr. Phys. **56**, 521 (2008); R. Horvat, A. Ilakovac, D. Kekez, J. Trampetić, and J. You, [arXiv:1204.6201](#).
- [15] T. Aaltonen *et al.* (CDF Collaboration), *Phys. Lett. B* **692**, 232 (2010).
- [16] ALEPH Collaboration, DELPHI Collaboration, L3 Collaboration, OPAL Collaboration, SLD Collaboration, LEP Electroweak Working Group, SLD Electroweak Group, and SLD Heavy Flavour Group, *Phys. Rep.* **427**, 257 (2006).
- [17] T. Aaltonen *et al.* (CDF Collaboration), *Phys. Rev. Lett.* **108**, 011801 (2012); *Phys. Lett. B* **717**, 173 (2012); K. R. Bland, Ph.D. thesis, Baylor University [Fermilab Report No. FERMILAB-THESIS-2012-11, 2012].
- [18] D. Acosta *et al.* (CDF Collaboration), *Phys. Rev. D* **71**, 032001 (2005).
- [19] T. Aaltonen *et al.*, *Nucl. Instrum. Methods Phys. Res., Sect. A* **729**, 153 (2013).
- [20] T. Affolder *et al.*, *Nucl. Instrum. Methods Phys. Res., Sect. A* **526**, 249 (2004).
- [21] L. Balka *et al.*, *Nucl. Instrum. Methods Phys. Res., Sect. A* **267**, 272 (1988); S. Bertolucci *et al.*, *Nucl. Instrum. Methods Phys. Res., Sect. A* **267**, 301 (1988); M. Albrow *et al.*, *Nucl. Instrum. Methods Phys. Res., Sect. A* **480**, 524 (2002).
- [22] CDF uses a cylindrical coordinate system with $+z$ in the proton beam direction. θ and ϕ are the polar and azimuthal angles, respectively, and pseudorapidity is $\eta = -\ln \tan(\theta/2)$.
- [23] G. Apollinari, K. Goulianos, P. Melese, and M. Lindgren, *Nucl. Instrum. Methods Phys. Res., Sect. A* **412**, 515 (1998).
- [24] The transverse energy E_T is defined as $E \sin \theta$.
- [25] T. Sjöstrand, P. Edén, C. Friberg, L. Lönnblad, G. Miu, S. Mrenna, and E. Norrbin, *Comput. Phys. Commun.* **135**, 238 (2001).
- [26] H. L. Lai, J. Huston, S. Kuhlmann, J. Morfin, F. Olness, J. F. Owens, J. Pumplin, and W. K. Tung, *Eur. Phys. J. C* **12**, 375 (2000).
- [27] R. Field and R. C. Group, [arXiv:hep-ph/0510198](#); T. Aaltonen *et al.* (CDF Collaboration), *Phys. Rev. D* **82**, 034001 (2010).
- [28] T. Aaltonen *et al.* (CDF Collaboration), *Phys. Rev. Lett.* **106**, 241801 (2011).
- [29] E. Gerchtein and M. Paulini, CDF Detector Simulation Framework and Performance, eConf C0303241, TUMT005 (2003). The version of GEANT used for the detector simulation is 3.21; see the CERN Program Library Long Writeup W5013.
- [30] T. Aaltonen *et al.* (CDF Collaboration), *Phys. Rev. Lett.* **103**, 061803 (2009).
- [31] T. Aaltonen *et al.* (CDF Collaboration), *Phys. Rev. D* **86**, 052010 (2012).
- [32] L. Lyons, *Ann. Appl. Stat.* **2**, 887 (2008).
- [33] D. Stump, J. Huston, J. Pumplin, W.-K. Tung, H.-L. Lai, S. Kuhlmann, and J. F. Owens, *J. High Energy Phys.* **10** (2003) 046; D. Bourilkov, R. C. Group, and M. R. Whalley, [arXiv:hep-ph/0605240](#).
- [34] We constrain the rate of initial-state radiation using Drell-Yan events in the data.